



## Climate impacts of the Atlantic Multidecadal Oscillation

Jeff R. Knight,<sup>1</sup> Chris K. Folland,<sup>1</sup> and Adam A. Scaife<sup>1</sup>

Received 8 March 2006; revised 12 May 2006; accepted 27 June 2006; published 2 September 2006.

[1] The Atlantic Multidecadal Oscillation (AMO) is a near-global scale mode of observed multidecadal climate variability with alternating warm and cool phases over large parts of the Northern Hemisphere. Many prominent examples of regional multidecadal climate variability have been related to the AMO, such as North Eastern Brazilian and African Sahel rainfall, Atlantic hurricanes and North American and European summer climate. The relative shortness of the instrumental climate record, however, limits confidence in these observationally derived relationships. Here, we seek evidence of these links in the 1400 year control simulation of the HadCM3 climate model, which produces a realistic long-lived AMO as part of its internal climate variability. By permitting the analysis of more AMO cycles than are present in observations, we find that the model confirms the association of the AMO with almost all of the above phenomena. This has implications for the predictability of regional climate. **Citation:** Knight, J. R., C. K. Folland, and A. A. Scaife (2006), Climate impacts of the Atlantic Multidecadal Oscillation, *Geophys. Res. Lett.*, *33*, L17706, doi:10.1029/2006GL026242.

### 1. Introduction

[2] Large multidecadal variations in regional climate have had significant impacts in the twentieth century. Some of these phenomena have been linked to multidecadal variations in Atlantic Sea Surface Temperatures (SSTs), particularly North East Brazilian (NEB) [Folland *et al.*, 2001] and African Sahel [Folland *et al.*, 1986; Rowell *et al.*, 1995; Rowell, 2003] rainfall, Atlantic hurricanes [Goldenberg *et al.*, 2001] and North American and European summer climate [Enfield *et al.*, 2001; McCabe *et al.*, 2004; Sutton and Hodson, 2005]. These SST variations have been called the 'Atlantic Multidecadal Oscillation' (AMO) and are part of a coherent temperature variation across much of the Northern Hemisphere [Knight *et al.*, 2005, hereinafter referred to as Kn05]. Cool AMO phases occurred in the 1900s–1920s and 1960s–1980s, while a warm phase occurred in the 1930s–1950s. These periods coincide with examples of anomalous regional climate: for example, the 1930s–1950s showed decreased NEB rainfall and United States (US) river flows, as well as enhanced Sahel rainfall and hurricane formation. Conversely, the 1960s–1980s were a period of high NEB rainfall and US river flows while Sahel rainfall and Atlantic hurricane formation were reduced.

[3] Kn05 showed that a 1400 year control simulation of the HadCM3 model captures a similar pattern, period and

amplitude to that seen in the few AMO phases contained in the instrumental data. This implies that the AMO is likely to be a long-lived quasi-periodic internal mode. Here, we utilise this successful simulation of the AMO to compare its regional climate links with those inferred from the relatively short observational period. Similar responses in the model would improve confidence in these relationships. Using an unforced coupled model rather than imposing the AMO via SSTs in an atmospheric model has the advantage of isolating the effects of internal variability, as observational estimates of the AMO cannot exclude a forced component with certainty. As in Kn05, we define an index of the AMO in the simulation and observations as the decadal filtered area-average North Atlantic (95°W–30°E, 0°–70°N, excluding the Mediterranean and Hudson Bay) SST anomaly after linear detrending.

### 2. North East Brazilian Rainfall

[4] Decadal variations of North East Brazil (NEB) wet season (March to May (MAM)) precipitation are strongly modulated by variations in the SST gradient between the north and south tropical Atlantic [Moura and Shukla, 1981; Hastenrath and Greischar, 1993; Folland *et al.*, 2001]. We use MTM-SVD analysis [Mann and Park, 1999] to examine links between surface air temperature and simulated MAM precipitation and 850 hPa winds. This technique derives the patterns of significant covariability at phases of a typical cycle within particular frequency bands. In the near-centennial AMO band [Kn05], the warm AMO phase (Figure 1a) is associated with a northward displacement of precipitation over the tropical Atlantic Ocean, along with a northward cross-equatorial wind anomaly (Figure 1e). These changes imply a shift in the mean inter-tropical convergence zone (ITCZ) to the north of its climatological MAM position, and hence a reduction in NEB rainfall. As the cycle of AMO phases proceeds, the temperature pattern eventually reverses (Figure 1d), forcing an anomalous southerly ITCZ located closer to NEB and so wetter decades (Figure 1h).

[5] The standard deviation of the decadal mean MAM NEB precipitation over nine decades of detrended observations between 1912–2001 is 48 mm, or about 11% of the mean. Simulated rainfall is derived from the closest grid points to the set of rainfall stations compiled by Hastenrath [Folland *et al.*, 2001]. Despite mean rainfall that is 40% less than observed, the variability is similar, with the decadal standard deviation averaging 39 mm and ranging from 24 to 58 mm in the 15 consecutive 9 decade sections of the simulation. Nine-decade correlations with the decadal AMO index in the model (average of  $-0.28$ ) similarly bracket the observed value ( $-0.39$ ), implying consistency between the simulated and observed links.

<sup>1</sup>Hadley Centre for Climate Prediction and Research, Met Office, Exeter, UK.

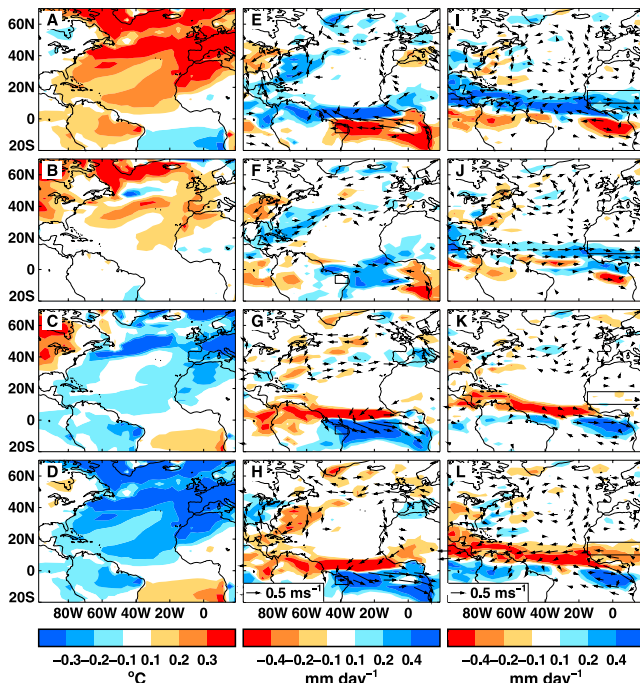


**Figure 1.** Joint MTM-SVD analyses of simulated decadal mean near-surface air temperature and decadal mean precipitation in the North Atlantic region for model years 400 to 900. Results from a joint analysis of (a–d) annual temperature and (e–h) March to May (MAM) precipitation are shown for the phases 0°, 60°, 120°, 180° of the signal detected in the frequency band from (70 years)<sup>-1</sup> to (180 years)<sup>-1</sup>. Zero phase is set to when mean Northern Hemisphere temperature is maximum. (i–l) Results for an equivalent analysis between annual temperature and June to August (JJA) precipitation. Surface temperature results from this second analysis are not shown due to their similarity to Figures 1a–1d. In addition, for each season 850 hPa wind anomalies in the same frequency band are displayed, determined from separate joint MTM-SVD analyses of temperature with each wind component. Plotting of vectors is suppressed where wind speed anomalies are small. The North East Brazil region is outlined in Figures 1e–1h, while the western Sahel region, including the Sudan (15°W–20°E, 10°–18°N), is outlined in Figures 1i–1l.

**3. Sahel Rainfall**

[6] Marked multidecadal variability of African Sahel rainfall is perhaps the best documented example of regional decadal climate variability [Nicholson *et al.*, 2000, and references therein]. We analyse the model results for the Sahel as for NEB, but for June to August (JJA) when much of the total annual rainfall occurs (Figures 1i–1l). Again, with a warm AMO phase (Figure 1a) tropical precipitation in the Atlantic sector shifts northward (Figure 1i). Along with consistent changes in the trade winds, this implies northward displacement of the mean ITCZ. Northward movement of the JJA climatological ITCZ brings increased precipitation to the Sahel. This coincides with anomalous westerly winds carrying moist Atlantic air into the region, as in previous studies [Rowell *et al.*, 1992]. In the opposite

phase, the ITCZ is displaced southward, away from the Sahel, resulting in below average rainfall (Figure 1j). While these results are qualitatively consistent with the observed sensitivity to the AMO, the simulated variability is considerably less. For the 10 decades between 1901 and 2000 the observed standard deviation of detrended rainfall (averaged over 15°W–37.5°E, 12.5°–17.5°N) is 39 mm, compared with a range of 11 to 26 mm (mean 19 mm) in 13 consecutive 10-decade sections of the simulation. The correlation with the AMO index, although significant, is also smaller (0.21) than in observations (0.83). Again, no 10-decade section has a correlation as large as in observations.

**4. Atlantic Hurricanes**

[7] Multidecadal variations in observed major hurricane activity in the period 1944 to 2000 have been associated with the AMO by Goldenberg *et al.* [2001]. They attribute this influence to changes in tropical atmospheric circulation which alter the tropospheric vertical shear in the main hurricane development region (MDR), with high shear reducing storm formation. Shear changes estimated from reanalysis data between positive and negative AMO decades show a band of reduced shear stretching across the Atlantic between approximately 10° and 20°N (Figure 2a), including

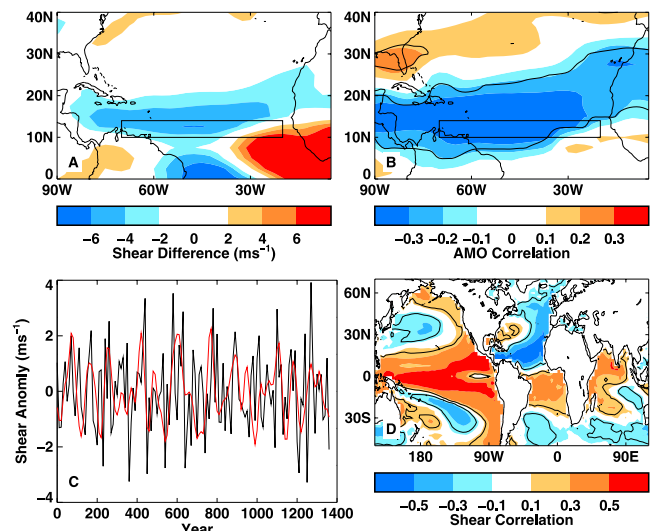


**Figure 2.** Relationship between the AMO and tropical Atlantic 850–200 hPa wind shear in reanalyses and the model simulation. (a) Difference between the mean August–October (ASO) shear between 1951–60 and 1971–80 derived from NCEP/NCAR reanalysis data. The section of the main Atlantic hurricane development region used by Goldenberg *et al.* [2001] (20°–70°W, 10°–14°N) is also shown. (b) Correlation between the simulated decadal AMO index and decadal tropical Atlantic shear. Contours indicate correlations significant at the 95% level accounting for auto-correlation. (c) Time series of the simulated mean decadal shear (black) in the box outlined in Figures 2a and 2b, together with the decadal AMO index filtered to retain time scales greater than 50 years (red). The AMO is scaled by 10 and reversed in sign. (d) Correlation between the simulated shear series in Figure 2c and global sea-surface temperatures. Again, contours indicate correlations significant at the 95% level accounting for auto-correlation.

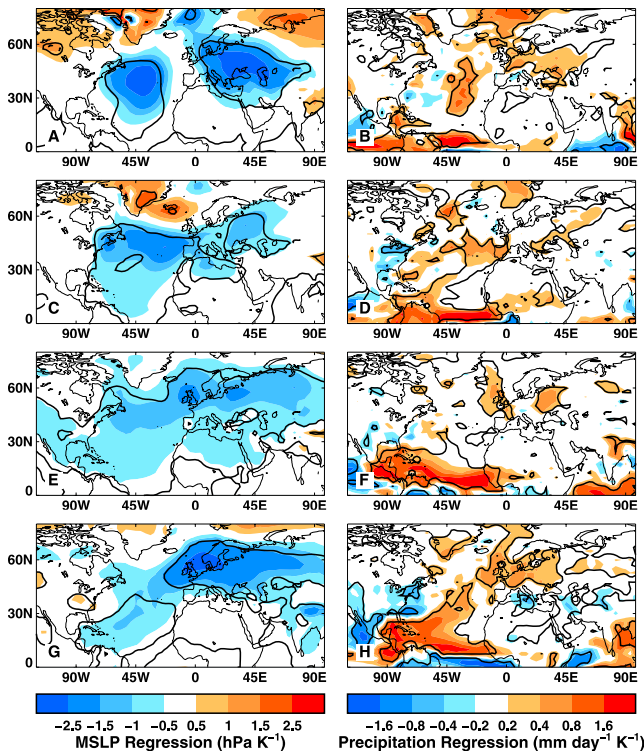


**Figure 3.** Simulated seasonal impact of the AMO on extratropical circulation and precipitation. (a and b) Regressions of the AMO index with decadal December–February (DJF) mean sea level pressure and precipitation respectively. Contours indicate correlations significant at the 90% level accounting for auto-correlation. The other panels show equivalent analyses for other seasons: (c and d) March–May (MAM), (e and f) June–August (JJA) and (g and h) September–November (SON).

most of the MDR (mean change of about  $4 \text{ m s}^{-1}$ ). The reliability of the observed AMO link is uncertain, however, being based on just one AMO cycle and from inherently inhomogeneous reanalysis data. Using the much longer model simulation shows a similar band of significant negative AMO correlations (Figure 2b), supporting a link with the AMO. Additionally, shear changes of several  $\text{m s}^{-1}$  are seen to occur at some transitions between AMO phases (Figure 2c), such as between years 400 and 450 of the simulation. The observed decadal anticorrelation with the AMO index for the 5 available decades ( $-0.81$ ) is larger than that in the simulation ( $-0.41$ ), although it still lies inside the range of correlations computed within consecutive 5-decade periods. The relationship of the simulated mean MDR shear with global SSTs shows negative correlations in the North Atlantic (Figure 2d), confirming the AMO link, but also shows significant positive correlations in the tropical Pacific. The Pacific pattern strongly resembles the model’s representation of the Interdecadal Pacific Oscillation [Power *et al.*, 1999], which has no significant correlation with the simulated AMO.

## 5. Mid-Latitude Climate

[8] Indications of AMO-related effects on summer climate over the US are seen in rainfall and river flow data

[Enfield *et al.*, 2001; McCabe *et al.*, 2004] and in atmospheric climate model simulations using prescribed historical SSTs [Sutton and Hodson, 2005]. Additionally, Sutton and Hodson [2005] show an effect on summer climate in North West Europe. In both cases, a positive AMO anomaly is related to decreased mean sea level pressure (mslp), but is associated with lower rainfall over the US and increased rainfall in North West Europe.

[9] We regress mslp and precipitation from our simulation with the AMO index to seek the mid-latitude responses in each season (Figure 3). For all seasons, positive AMO conditions favour broad cyclonic pressure anomalies over the Atlantic and Europe. The amplitude of pressure changes is greatest in winter (DJF), although they are most widespread in summer (JJA), encompassing North Africa and parts of North America. These patterns closely resemble the observed seasonal AMO-mslp relations shown by Kushnir [1994], although with somewhat less amplitude. In addition, the JJA pattern is similar to that of Sutton and Hodson [2005], except that the largest signal is seen over the US in their study. Patterns of rainfall change are more sporadic and seasonally variable. Overall, there is a tendency for increased rainfall over the Atlantic with the positive AMO. In JJA, significant rainfall changes appear to be connected with cyclonicity changes over North West Europe, but the observed signal in US rainfall is absent. The model hints at US rainfall changes in SON, and shows its strongest impact on Northern European precipitation.

[10] These results show a seasonal dependence of AMO climate impacts on the North West European region. To gauge this further, we examine 1871–1999 correlations (Table 1) between the AMO and Central England Temperature (CET) [Parker and Horton, 2005]. The observed correlations are only significant in JJA and SON, when they have their highest positive values. The length of the model simulation allows a much lower threshold for significance, and shows significant positive correlations in all seasons. Despite this, the strongest correlations are again in JJA and SON, and agree well with those derived from observations. In these seasons, the AMO can explain 30–40% of the observed low frequency CET variance, with regression coefficients showing temperature fluctuations of 1.3 (JJA) and 1.1 (SON) times those of the AMO. In the simulation, the regressions are similar, with signals 1.5 (JJA) and 1.3 (SON) times the AMO. Regressions for consecutive

**Table 1.** Correlations Between the AMO Index and Observed [Parker and Horton, 2005] and Simulated Central England Temperature (CET)<sup>a</sup>

	Observed	Simulated
DJF	-0.35	<b>+0.31</b>
MAM	+0.39	<b>+0.26</b>
JJA	<b>+0.53</b>	<b>+0.50</b>
SON	<b>+0.61</b>	<b>+0.41</b>
Annual	+0.32	<b>+0.52</b>

<sup>a</sup>The observed 1871–1999 CET is detrended and low-pass filtered to retain time scales longer than 13.3 years. Simulated CET is taken as the surface temperature of the closest model grid-point and the correlation performed with decadal mean data. Correlations shown in bold are significant at the 95% confidence limit after accounting for serial auto-correlation.

13-decade periods show that the observed amplitudes are consistent with the range of those simulated.

## 6. Discussion and Conclusions

[11] We have shown that the HadCM3 control simulation reproduces most of the AMO climate impacts inferred from short instrumental records. This gives greater confidence in the physical basis of some of the supposed links, and implies that they are likely to be a persistent feature of AMO variability.

[12] The size of the apparent reduction in NEB rainfall between negative and positive AMO phases is well simulated in the model and shown to be related to multidecadal shifts in the position of the mean MAM ITCZ. Similarly, reductions in Sahel rainfall are shown to occur in negative AMO phases due to southward shifts in the JJA mean ITCZ. The simulated amplitude of Sahel rainfall variations is, however, considerably smaller than observed. This may be due in part to the approximately 40% smaller amplitude of simulated AMO SST anomalies [Kn05], and additional multidecadal influences from SSTs outside the Atlantic [Giannini *et al.*, 2003; Lu and Delworth, 2005]. Despite this, the atmospheric component of the model does not reproduce the magnitude of Sahel rainfall variability when forced with global historical SSTs, suggesting model deficiencies also have a role.

[13] The model results also provide physical evidence for the observed link between the AMO and tropospheric vertical shear in the main hurricane development region. Simulated correlations are consistent with those derived from reanalyses, implying the AMO may explain at least part of the observed multidecadal variability in hurricane activity. This does not preclude, however, the possibility of an influence from anthropogenic climate change [Emanuel, 2005]. The model results also show an association of hurricane region shear with multidecadal variations in Pacific SSTs.

[14] Patterns of increased extratropical cyclonicity and rainfall over parts of the Atlantic region are simulated for positive AMO phases in all seasons and resemble those estimated from observations. The largest amplitudes are found in winter, but the most widespread impact occurs in summer. The model does not reproduce the observed anticorrelation with JJA rainfall in the US, but shows some signal in SON. Climate effects on North West Europe, as gauged by positive correlations with simulated rainfall and CET, also peak in JJA and SON. The results imply an AMO influence in all seasons, but that JJA offers the best chance of detection in observations due to a larger signal-to-noise ratio.

[15] Kn05 provided evidence that the AMO is related to variations in the strength of the overturning circulation in the Atlantic Ocean and may be potentially predictable several decades ahead. Here, our results show that this

predictability could be extended to a range of key regional climate impacts.

[16] **Acknowledgments.** The authors acknowledge the UK Government Meteorological Research (GMR) programme, the EU-sponsored EMULATE project, and the CLIVAR International Climate of the Twentieth Century project.

## References

- Emanuel, K. (2005), Increasing destructiveness of tropical cyclones over the past 30 years, *Nature*, *436*, 686–688.
- Enfield, D. B., A. M. Mestas-Núñez, and P. J. Trimble (2001), The Atlantic multidecadal oscillation and its relation to rainfall and river flows in the continental US, *Geophys. Res. Lett.*, *28*, 2077–2080.
- Folland, C. K., D. E. Parker, and T. N. Palmer (1986), Sahel rainfall and worldwide sea temperatures, 1901–85, *Nature*, *320*, 602–607.
- Folland, C. K., A. W. Colman, D. P. Rowell, and M. K. Davey (2001), Predictability of northeast Brazil rainfall and real-time forecast skill, 1987–98, *J. Clim.*, *14*, 1937–1958.
- Giannini, A., R. Saravanan, and P. Chang (2003), Oceanic forcing of Sahel rainfall on interannual to interdecadal time scales, *Science*, *302*, 1027–1030.
- Goldenberg, S. B., C. W. Landsea, A. M. Mestas-Núñez, and W. M. Gray (2001), The recent increase in Atlantic hurricane activity: Causes and implications, *Science*, *293*, 474–479.
- Hastenrath, S., and L. Greischar (1993), Circulation mechanisms related to northeast Brazil rainfall anomalies, *J. Geophys. Res.*, *98*, 5093–5102.
- Knight, J. R., R. J. Allan, C. K. Folland, M. Vellinga, and M. E. Mann (2005), A signature of persistent natural thermohaline circulation cycles in observed climate, *Geophys. Res. Lett.*, *32*, L20708, doi:10.1029/2005GL024233.
- Kushnir, Y. (1994), Interdecadal variations in North Atlantic sea surface temperature and associated atmospheric conditions, *J. Clim.*, *7*, 141–157.
- Lu, J., and T. L. Delworth (2005), Oceanic forcing of the late 20th century Sahel drought, *Geophys. Res. Lett.*, *32*, L22706, doi:10.1029/2005GL023316.
- Mann, M. E., and J. Park (1999), Oscillatory spatiotemporal signal detection in climate studies: A multiple-taper spectral domain approach, *Adv. Geophys.*, *41*, 1–131.
- McCabe, G. J., M. A. Palecki, and J. L. Betancourt (2004), Pacific and Atlantic Ocean influences on multidecadal drought frequency in the United States, *Proc. Natl. Acad. Sci. U. S. A.*, *101*, 4136–4141.
- Moura, A. D., and J. Shukla (1981), On the dynamics of droughts in northeast Brazil: Observations, theory and numerical experiments with a general circulation model, *J. Atmos. Sci.*, *38*, 2653–2675.
- Nicholson, S. E., B. Some, and B. Kone (2000), An analysis of recent rainfall conditions in West Africa, including the rainy seasons of the 1997 El Niño and the 1998 La Niña years, *J. Clim.*, *13*, 2628–2640.
- Parker, D. E., and E. B. Horton (2005), Uncertainties in the Central England Temperature series 1878–2003 and some improvements to the maximum and minimum series, *Int. J. Climatol.*, *25*, 1173–1188.
- Power, S., T. Casey, C. Folland, A. Colman, and V. Mehta (1999), Interdecadal modulation of the impact of ENSO on Australia, *Clim. Dyn.*, *15*, 319–324.
- Rowell, D. P. (2003), The impact of Mediterranean SSTs on the Sahelian rainfall season, *J. Clim.*, *16*, 849–862.
- Rowell, D. P., C. K. Folland, K. Maskell, J. A. Owen, and M. N. Ward (1992), Modelling the influence of global sea-surface temperatures on the variability and predictability of seasonal Sahel rainfall, *Geophys. Res. Lett.*, *19*, 905–908.
- Rowell, D. P., C. K. Folland, K. Maskell, and M. N. Ward (1995), Variability of summer rainfall over tropical North-Africa (1906–92) observations and modelling, *Q. J. R. Meteorol. Soc.*, *121*, 669–704.
- Sutton, R. T., and D. L. R. Hodson (2005), Atlantic Ocean forcing of North American and European summer climate, *Science*, *309*, 115–118.

C. K. Folland, J. R. Knight, and A. A. Scaife, Hadley Centre for Climate Prediction and Research, Met Office, FitzRoy Road, Exeter, EX1 3PB, UK. (jeff.knight@metoffice.gov.uk)